Available at www.sciencedirect.com

ScienceDirect

journal homepage: www.elsevier.com/locate/watres

Real-time microgravimetric quantification of *Cryptosporidium parvum* in the presence of potential interferents

*Charles Poitras, Julien Fatisson, Nathalie Tufenkji**

Department of Chemical Engineering, McGill University, Montreal, Quebec, Canada H3A 2B2

ARTICLE INFO

Article history:
Received 4 February 2009
Received in revised form
12 March 2009
Accepted 15 March 2009
Published online 21 March 2009

Keywords:
QCM-D
C. parvum
Interference
Dissipation slope
Biosensor

ABSTRACT

The quartz crystal microbalance with dissipation monitoring (QCM-D) is used to develop a biosensor for detection of viable *Cryptosporidium parvum* (*C. parvum*) in water matrices of varying complexity. In a clean environment, a good log–log linear response is obtained for detection of *C. parvum* in aqueous suspensions with oocyst concentrations from 3×10^5 to 1×10^7 oocysts/mL. *C. parvum* detection is slightly affected by the presence of dissolved organic acids, likely due to steric stabilization and/or masking of the antibodies/antigens by adsorbed molecules. Colloidal contaminants generally have a greater influence as biosensor interferents, whereby the presence of model latex microspheres, *Enterococcus faecalis*, or *Escherichia coli*, led to decreases in biosensor response of up to 64%, 40%, and 20%, respectively.

1. Introduction

Cryptosporidium parvum (*C. parvum*) has emerged as one of the most important microbial pathogens for drinking water safety and is associated with a high risk of waterborne illness (Rose, 1997). The protozoan parasite *C. parvum* is commonly transmitted via the faeces of infected mammalian hosts in the form of an oocyst which is highly resistant to environmental stresses (Smith, 1992). Ingestion of a small number of viable oocysts (as little as 10) can lead to cryptosporidiosis, a diarrheal disease that is potentially lethal for immunosuppressed individuals (Casemore et al., 1997; Rose, 1997). Several outbreaks of cryptosporidiosis related to drinking water contamination have been reported in Europe and North America over the past 20 years (Lisle and Rose, 1995; Smith and Perdek, 2004). The public health risk posed by *C. parvum* underscores the need to develop rapid and reliable sensors for detection of the parasite in potable water supplies.

Various approaches have been proposed for detection of *C. parvum* in water samples, including conventional microscopy, immunological assays, flow cytometry, and nucleic-acid based methods (Jex et al., 2008). These methods require varying extents of sample preparation, concentration, and/or labeling, and exhibit different levels of detection. For example, the commonly used US EPA method 1623 requires filtration, immunomagnetic separation of the oocysts, and an immunofluorescence assay with confirmation via differential interference contrast microscopy (Jex et al., 2008). Recently, a piezoelectric-excited millimeter-sized cantilever (PEMC) sensor has successfully been used to detect *C. parvum* oocysts at concentrations as low as 100 oocysts/mL in less than 1 min (Campbell and Mutharasan, 2008). The quartz crystal microbalance (QCM) functions in a manner analogous to PEMC biosensors but has not previously been considered for detection of *C. parvum*. Hence, it is of interest to evaluate the potential use of QCM in direct, real-time detection of *C. parvum*.

* *Corresponding author*. Tel.: +1 514 398 2999; fax: +1 514 398 6678.
E-mail address: nathalie.tufenkji@mcgill.ca (N. Tufenkji).
0043-1354/$ – see front matter © 2009 Elsevier Ltd. All rights reserved.
doi:10.1016/j.watres.2009.03.021

A major challenge associated with detection of target microorganisms is interference by dissolved substances or particulates present in the water samples. Organic matter, microbial exudates, and colloidal particles (including a broad range of microorganisms) are commonly found in untreated surface waters and groundwater supplies and may interfere with biosensor performance. However, few studies of biosensor development consider the potential influence of dissolved and/or colloidal contaminants on pathogen detection in complex matrices (Campbell et al., 2007; Edgar et al., 2006; Kang et al., 2008; Subramanian et al., 2006; Waswa et al., 2006). Some researchers have evaluated biosensor interference by non-target organisms (Lee et al., 2005; Su and Li, 2005, 2004; Vaughan et al., 2001), however, the potential influence of non-biological colloids using model particles has not been examined in previous studies of biosensor development. Another important difficulty in evaluating the occurrence of waterborne pathogens such as *C. parvum* is the relatively low environmental concentrations in contaminated water supplies (~0.1–10 oocysts/L) (Mons et al., 2009).

The purpose of this study is to examine the potential interference of a biosensor based on a quartz crystal microbalance with dissipation monitoring (QCM-D) by natural organic matter (NOM) and model colloids (including bacteria) that may be found in natural waters. Antibodies immobilized onto a gold-coated QCM-D crystal were used for rapid detection of viable *C. parvum* oocysts over a range of concentrations. Experiments conducted in the presence of NOM demonstrate some interference, whereas colloidal contaminants generally yield larger decreases in the biosensor response.

2. Materials and methods

2.1. Reagents

Mouse monoclonal immunoglobulin M (IgM), specific to *C. parvum*, was obtained from Waterborne Inc., New Orleans, LA. Bovine serum albumin (BSA) and phosphate buffer saline (PBS) tablets were purchased from Sigma–Aldrich. Suwannee river humic acid (SRHA) and Suwannee river fulvic acid (SRFA) standards (International Humic Substances Society, St. Paul, MN) were dissolved in PBS. Surfactant-free polystyrene latex microspheres (1.5 μm diameter) with sulfate functional groups (Interfacial Dynamics Microspheres and Nanospheres, Eugene, OR) were suspended in PBS at a concentration of 5×10^6 particles/mL. Denatured alcohol (Fisher Scientific, Canada), Hellmanex (Hellma, Thornhill, ON), hydrogen peroxide (Fisher), and ammonia (LabChem Inc., ON) were used to clean the crystal surfaces after each experiment. Ultrapure deionized (DI) water was used to prepare all PBS solutions (Biolab).

2.2. Preparation of oocysts and bacteria

Viable oocysts were obtained from the Sterling Parasitology Laboratory (SPL) at the University of Arizona. The oocysts were shed from a calf infected with the Iowa isolate from Dr. Harley Moon (National Animal Disease Center, Ames, Iowa). Oocysts were purified (at SPL) using discontinuous sucrose and cesium chloride centrifugation gradients and stored (in the dark at 4 °C) in an antibiotic solution (0.01% Tween 20, 100 U of penicillin, and 100 μg of gentamicin per mL). Before conducting experiments, oocysts were pelleted by centrifugation (9300*g* for 2 min, IEC MicroCL 17R, Thermo) and the supernatant was replaced with 1 mL PBS. This step was repeated twice to remove any trace of the antibiotic solution. Purified oocysts were diluted to the desired concentration in PBS (pH 7.4) prior to the QCM-D experiments. The oocyst concentration was determined using a cell counting chamber (Hawksley Medical and Lab Equipment, Lancing, UK).

Escherichia coli (*E. coli*) O157:H7 (ATCC 700927) and *Enterococcus faecalis* (*E. faecalis*) (ATCC 29212) were used as representative interfering pathogenic organisms. *E. coli* O157:H7 is a Gram-negative bacterium while *E. faecalis* is a Gram-positive organism. Pure cultures were maintained at −80 °C in Luria–Burtani (LB) Lennox broth (Fisher Scientific, Canada) (20 g/L) containing 15% glycerol. Pure cultures were then streaked onto LB agar followed by 24 h incubation at 37 °C. For interference experiments using bacteria, colonies from a fresh plate were used to inoculate 150 mL of LB broth (in a 500 mL baffled flask). Liquid cultures were incubated at 37 °C for 18 h at 200 rpm. The bacterial suspension was harvested by centrifugation (Sorvall RC6, Thermo Scientific, Waltham, MA) at 5860*g* in a SS34 rotor (Kendro, Thermo Scientific, Waltham, MA) at 4 °C. The bacterial pellet was re-suspended in PBS at pH 7.4. The centrifugation and re-suspension steps were repeated one additional time to remove any traces of growth media. The resulting bacterial cell concentration (total cells) was determined using the same cell counting chamber (Hawksley Medical and Lab Equipment).

For interference experiments, the following suspensions were prepared: (i) mixture of *C. parvum* (5×10^6 oocysts/mL) and *E. coli* (5×10^6 cells/mL); (ii) mixture of *C. parvum* (5×10^6 oocysts/mL) and *E. faecalis* (5×10^6 cells/mL); (iii) mixture of *C. parvum* (5×10^6 oocysts/mL) and latex microspheres (5×10^6 particles/mL); (iv) *C. parvum* (5×10^6 oocysts/mL) in PBS supplemented with 1 mg/L SRHA or SRFA.

2.3. Detection of Cryptosporidium using QCM-D

A quartz crystal microbalance with dissipation monitoring (QCM-D) was used as a platform to monitor binding of *C. parvum* and/or the interfering agents to an antibody covered gold-coated crystal surface. QCM-D differs from traditional QCM in that it gives insight into the viscoelastic properties of the adsorbed mass. The fundamental concept of the QCM-D technology is that a ''soft'' mass adhered to the crystal surface will not fully couple to the crystal's oscillation and thus will dampen it (Hook, 1997). The energy dissipation factor *D* represents the sum of all processes that induce energy losses in the oscillating system (Hook, 1997). The E4 QCM-D unit (Q-Sense AB, Västra Frölunda, Sweden) consists of a measurement platform that can hold 4 sensor flow chambers with a volume of 40 μL each. The flow chambers were maintained at 20 °C during experiments. Clean gold-coated QCM-D crystals (QSX 301, 5 MHz, AT-cut, Q-Sense AB) were mounted inside the flow modules. PBS (pH 7.4) was injected for 10 min (50 μL/min) using a peristaltic pump (Reglo-Digital

IPC-N4, Ismatec SA, Glattbrugg, Switzerland) to ensure that stable baselines in frequency (f) and energy dissipation (D) shifts were achieved. A suspension of anti-*C. parvum* antibodies (10 μg/mL) in PBS was injected into each flow chamber for 20 min at a flow rate of 50 μL/min. The pump was then stopped for a duration of 60 min to allow time for the antibody to physically adsorb to the gold surface. This step was followed by a 20 min PBS rinse under flow to remove any unbound antibody. Next, a BSA solution in PBS (10 mg/mL) was injected for 20 min (50 μL/min) to block non-specific sites, and the pump was stopped for 60 min before a 20 min PBS rinse to remove any unbound BSA. The prepared sensors were then ready for detection of the target organism. A suspension of *C. parvum* or mixture of *C. parvum* and bacteria/microspheres was then injected for a period of 10 min (50 μL/min) after which the pump was stopped for 60 min to allow sufficient time for oocyst attachment to the antibody-coated surface. A final 20 min PBS rinse was then performed. Shifts in the crystal frequency and energy dissipation for the first overtone were continuously monitored at each experimental step using Q-Soft software (Q-Sense AB). Following each experiment, the QCM-D crystals were imaged (see Section 2.4) then cleaned using the following procedure: the crystals were (i) sonicated for 5 min in denatured alcohol (ii), sonicated for 5 min in the presence of 2% Hellmanex, (iii) rinsed thoroughly with DI water, (iv) soaked in a hot mixture (85 °C) of 30% H_2O_2, ammonia, and DI water, at a 1:1:5 ratio, (v) rinsed with DI water, and (vi) dried with ultra-high purity (UHP) N_2. Each experiment was conducted with a clean gold-coated crystal and required the antibody adsorption step prior to the detection step. ''Because the dissipation factor (D) is a ratio of energies, it is dimensionless and is reported as 10^{-6} dissipation units (DU).''

2.4. *Optical and electron microscopy*

Following each QCM-D experiment, the gold-coated crystals were gently rinsed with DI water, and dried under a stream of UHP N_2. The crystals were then imaged using optical microscopy (IX-71, Olympus) and images analyzed using ImageJ software.

High resolution images of *C. parvum* oocysts were obtained using a Hitachi S-4700 Field Emission Gun Scanning Electron Microscope (FEG-SEM). A suspension of oocysts (10 μL) was pipetted onto a gold-coated glass slide and left to sit for 1 h to allow oocyst binding. The slides were then rinsed with PBS, and the oocysts were fixed twice overnight with 2.5% glutaraldehyde in PBS (pH 7.4). The samples were then dehydrated using ethanol/water solutions of increasing ethanol content from 30% to 100% and amyl acetate/ethanol solutions, with increasing amyl acetate content from 25% to 100%. Dehydration was followed by a critical point drying step (LADD Research Industries) and the slides were finally coated with Au/Pd prior to imaging.

3. Results and discussion

3.1. Cryptosporidium *detection in a clean water matrix*

Preliminary experiments were carried out to evaluate two approaches for immobilization of anti-*C. parvum* antibodies to the gold-coated quartz crystal surface. Direct physisorption of the pentamer-shaped antibodies was conducted as described in Section 2.3. Immobilization of antibodies via a cysteamine self-assembled monolayer (as described in Poitras and Tufenkji, 2009) was also considered. The f and D shifts measured after binding of *C. parvum* oocysts to the physisorbed or chemically immobilized antibodies were nearly identical. Hence, for simplicity, physisorption was selected as the method for antibody immobilization on the gold-coated crystal surface.

Shifts in the resonance frequency (f) and dissipation factor (D) were monitored during injection of the antibody solution (10 μg/mL) into the QCM-D flow chambers (Fig. 1). At the end of phase I, the resonance frequency (f) had reached a stable value of -45.81 ± 0.05 Hz, indicating an increase in adhered mass at the crystal surface. Correspondingly, at the end of phase I, the energy dissipation factor (D) had reached a plateau at 2.42 ± 0.01 DU.

To reduce non-specific binding of organisms to the antibody layer, BSA was used as a blocking agent. During injection of BSA into the flow modules (phase II in Fig. 1), a negative shift in f and a positive shift in D were observed, as previously shown for protein adsorption (Dolatshahi-Pirouz et al., 2008; Hook et al., 2002; Nimeri et al., 1998). During injection of BSA,

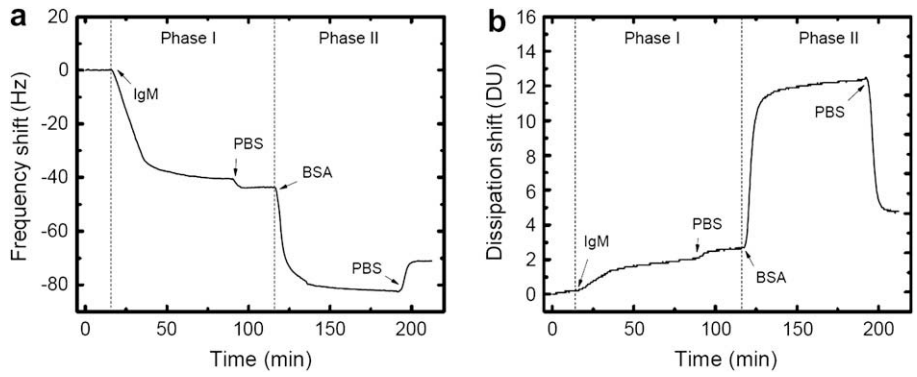

Fig. 1 – QCM-D measurements of the 1 overtone (a) frequency and (b) dissipation shifts during physisorption of anti-*C. parvum* antibodies onto gold-coated quartz crystals (phase I) followed by BSA adsorption (phase II).

the measured shift in the resonance frequency (Δf) was -20.51 ± 0.07 Hz, corresponding to an increase in adhered mass onto the crystal. During phase II, the total shift in the energy dissipation factor (ΔD) was 1.46 ± 0.01 DU. Model calculations of the QCM-D data using QTools software (Q-Sense AB) predict a thickness of 3.40 ± 0.01 nm for the BSA layer, which is slightly greater than the shorter ellipsoidal axis of an albumin molecule (3 nm × 8.2 nm × 8.5 nm) (Hook et al., 1998). In these calculations, the density of the antibody layer was estimated as 1.35 g/cm^3 (Hook et al., 2001, 2002). The model calculations should be considered with caution however since the adsorbed layer can also be composed of rigidly associated water. Moreover, BSA likely does not form a uniform monolayer above the layer of antibodies as assumed in the model calculations (Tencer et al., 2007). Nevertheless, this result suggests that BSA conformation upon adsorption onto the crystal is more likely to be horizontal than vertical as has been previously reported for deposition onto polystyrene and silica surfaces (Green et al., 1997; Kim and Somorjai, 2003). The calculated mass of BSA on the crystal surface (459 ng/cm^2) is in accordance with previous studies (Hook et al., 2002; Lubarsky et al., 2007). Hook et al. (2002) obtained a value of 333 ng/cm^2 albumin coverage from a much more dilute solution (80 μg/mL). Our result is also comparable to that obtained by Lubarsky et al. (2007) who reported a BSA thickness of nearly 3 nm, corresponding to a mass of 405 ng/cm^2.

Fig. 2 shows an SEM image of an intact *C. parvum* oocyst on the surface of a gold-coated slide. The oocyst is nearly 3 μm in diameter and is spherical in shape. Representative f and D shifts measured during injection of a suspension of *C. parvum* oocysts are presented in Fig. 3. When oocysts are injected over the antibody covered gold-coated crystal, both the resonance frequency (f) and energy dissipation factor (D) increase with time. According to Sauerbrey (1959), an increase in attached mass on the crystal surface is reflected by a decrease in the resonance frequency of the crystal. However, the data in Fig. 3 show an opposite behavior whereby a positive shift in f is detected during *C. parvum* injection. Previous QCM studies using *Salmonella*, *E. coli*, *Listeria*, and metal oxide nanoparticles (Fatisson et al., in press; Poitras and Tufenkji, 2009; Su and Li, 2005; Vaughan et al., 2001) have suggested that the observed positive frequency shifts may be attributed to the accumulation of weakly attached particles at the liquid–crystal interface or the formation of thick viscoelastic films on the crystal surface, while negative frequency shifts are normally expected when stronger interactions are involved. Both the measured f and D shifts increase with increasing oocyst concentration while the control experiment (PBS with no oocysts) exhibits no change in f or D. Hence, the raw data presented in Fig. 3 suggest that the QCM-D measurements provide real-time sensing of *C. parvum* oocysts in suspension.

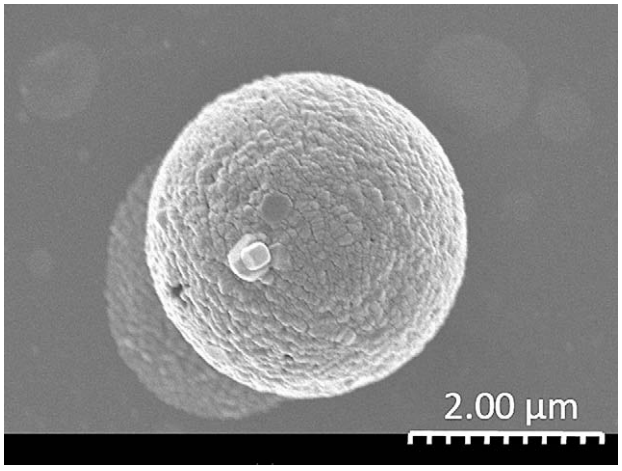

Fig. 2 – FEG-SEM image of a *C. parvum* oocyst (20,000× magnification) adhered onto a gold-coated glass slide.

Other studies of QCM based biosensors (Mao et al., 2006; Shen et al., 2007; Su and Li, 2005, 2004; Vaughan et al., 2001; Wong et al., 2002) have reported dose–response relationships based on the measured f shift after stabilization of the QCM signal. In our earlier work (Poitras and Tufenkji, 2009), we demonstrated the value of calculating the initial slopes in the measured f and D shifts as a function of time as important biosensor signals. The values of f_{slope} and D_{slope} can represent the rate of change of mass or energy loss at the crystal surface which are related to the rate of particle/microbe attachment. One advantage of using these parameters as biosensor responses is that one does not need to wait for the signal to stabilize (i.e., reach a plateau). Hence, the measurement of the initial f_{slope} and D_{slope} can provide a rapid means to evaluate the biosensor response (Poitras and Tufenkji, 2009) as only the first few minutes of detection are needed.

Fig. 4 presents the calculated values of the initial f_{slope} and D_{slope} when suspensions of *C. parvum* at different oocyst concentrations were injected into the QCM-D flow chambers. The open symbols represent measurements obtained using suspensions of *C. parvum* in PBS alone. In the absence of potential interfering agents, the calculated values of f_{slope} exhibit a log–log linear increase ($R^2 = 0.99$) as a function of oocyst concentration, from a concentration of 3×10^5 oocysts/mL to a maximum tested limit of 10^7 oocysts/mL (Fig. 4a). Likewise, the data show a log–log linear increase in D_{slope} ($R^2 = 0.99$) over the same range of injected oocyst concentrations (Fig. 4b). Below a concentration of 3×10^5 oocysts/mL, the f and D shifts could not be distinguished from the baseline signals and the measured drift of the instrument; hence, these data cannot be included in Fig. 4 which is in a log–log scale. The maximum oocyst concentration evaluated was 10^7 oocysts/mL. In our earlier work, we found that the D_{slope} was a better choice of biosensor response signal than the f_{slope} (Poitras and Tufenkji, 2009) for detection of *E. coli* O157:H7. In the present study with *C. parvum* oocysts, it can be noted that the response behavior of the biosensor is similar for both the f_{slope} and the D_{slope}.

Various approaches have been used for detection of *C. parvum* oocysts in complex matrices. Robinson et al. (2008) proposed a method allowing detection of less than 5 oocysts per gram of human faeces. However, their approach necessitates sample preparation by immunomagnetic separation and oocyst labeling for detection by fluorescence microscopy. Barbosa et al. (2008) used flow cytometry to detect *C. parvum* oocysts in stool with a sensitivity of 2×10^3 oocysts/mL, but their protocol also required sample preparation and labeling. Kang et al. (2008, 2006) employed surface plasmon resonance to achieve a sensitivity as low as 10^2 oocysts/mL when various

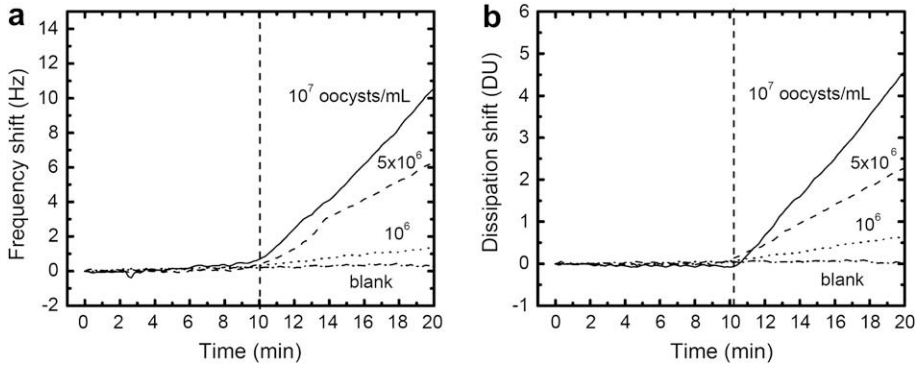

Fig. 3 – Representative QCM-D measurements of the 1 overtone (a) frequency and (b) dissipation shifts for binding of *C. parvum* to antibody modified gold-coated quartz crystal. Phase I: baseline in PBS; phase II: *C. parvum* oocysts suspended in PBS (pH 7.4) are injected at different concentrations: 10^7 oocysts/mL (solid lines), 5×10^6 oocysts/mL (dashed lines), 10^6 oocysts/mL (dotted lines) and no oocyst (dashed dotted lines).

oocyst preparation methods were utilized. Recently, Campbell and Mutharasan (2008) reported rapid detection (~1 min) and low detection limits for *C. parvum* (between 10^2 and 10^5 oocysts/mL in a clean PBS matrix) by using piezoelectric cantilevers. QCM-D provides similar advantages to the piezoelectric cantilever approach. Use of the initial f_{slope} and D_{slope} as biosensor responses provides for rapid detection as these values are calculated from the frequency (f) and energy dissipation (D) measurements during the first few minutes of oocyst injection into the flow chamber. Using this approach, there is no need to wait for a stable plateau to be reached in the QCM-D response (i.e., the frequency or dissipation shifts). Hence, *C. parvum* detection can be confirmed very rapidly with this approach. Moreover, the proposed technique does not require labeling of the oocysts for detection.

A series of experiments were conducted to confirm that the measured f and D shifts correspond to specific binding of oocysts with the antibody layer on the crystal surface. These control experiments were conducted using crystals that were prepared without the addition of antibody. When these "no antibody" crystals were exposed to a suspension of *C. parvum* oocysts (10^7), no measurable shifts in f or D were observed. In addition, following each experiment, the crystals were removed from the flow chambers, rinsed with DI water, dried, and viewed by optical microscopy. Fig. 5a shows an optical microscopy image of a QCM-D crystal prepared with physisorbed antibody and BSA and exposed to *C. parvum* (5×10^6 oocyst/mL) for 60 min. The image shows abundant coverage of *C. parvum* oocysts on the crystal surface. In contrast, the crystal prepared without antibody reveals very little binding of *C. parvum* on the sensing surface (Fig. 5b). Hence, the measured f and D shifts can be attributed to specific binding of the oocysts to the layer of physisorbed antibodies.

3.2. *Cryptosporidium* detection in the presence of non-biological interferents

Many studies reporting the development of biosensors for microbial pathogens such as *C. parvum* neglect the potential interference caused by other suspended particles (e.g., non-biological colloids) or dissolved macromolecules such as organic acids or extracellular polymeric substances (Campbell and Mutharasan, 2008; Kang et al., 2006; Subramanian et al., 2006; Wong et al., 2002). We conducted QCM-D experiments to evaluate the potential interference caused by humic and fulvic acids which are common organic macromolecules found in surface waters and groundwaters that may be contaminated by microbial pathogens. The results of experiments conducted in the presence of 1 mg/L SRHA or SRFA are

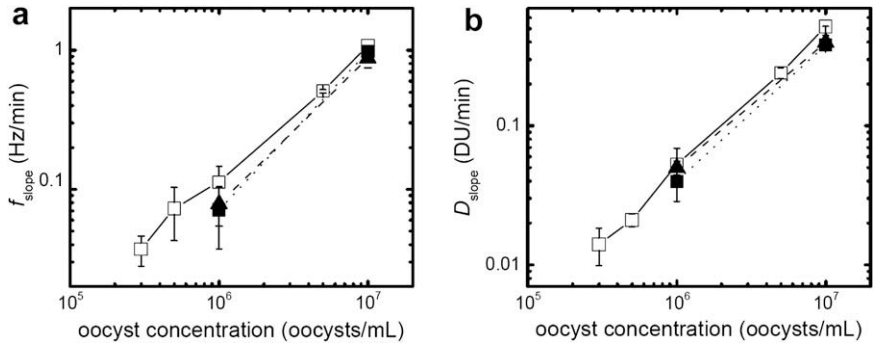

Fig. 4 – Average values of (a) f_{slope} and (b) D_{slope} measured during injection of *C. parvum* into the QCM-D flow modules as a function of oocyst concentration: (□) in PBS alone, (▲) in the presence of 1 mg/L SRHA, and (■) in the presence of 1 mg/L SRFA. Error bars correspond to 95% confidence intervals for at least 3 separate experiments.

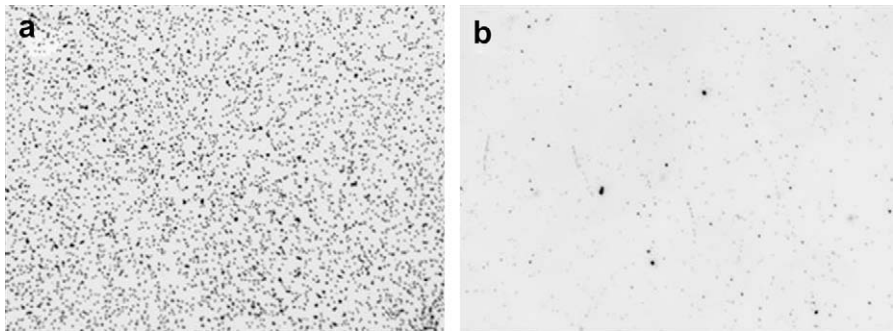

Fig. 5 – 4× Magnification light-microscopy images of (a) sensor prepared with antibody and BSA, and (b) sensor prepared without antibody after exposure to 60 min injection of *C. parvum* oocysts (5×10^6 oocysts/mL). The negative of the microscope images are presented for improved clarity (*i.e.*, oocysts are shown as black spots on a white background).

presented in Fig. 4 as solid symbols. For the two tested concentrations of *C. parvum*, the biosensor response (i.e., measured values of f_{slope} and D_{slope}) in the presence of the organic acids is generally very close to that obtained under ''clean'' conditions (open symbols); however, the response does decrease for some of the conditions (e.g., Fig. 4a, 1 mg/L SRFA). Humic and fulvic acids can adsorb onto the surface of microorganisms or non-biological colloids (Dai and Hozalski, 2003; Franchi and O'Melia, 2003) resulting in increased negative charge. Indeed, many studies have shown that NOM can adsorb onto the surface of *C. parvum* oocysts thereby rendering them more negative (Dai and Hozalski, 2003; Tufenkji et al., 2006). This greater negative charge on the oocyst surface may lead to increased repulsive electrical double-layer interactions upon approach of the oocyst to the QCM crystal surface (Derjaguin and Landau, 1941; Verwey and Overbeek, 1948). Although this phenomenon may be partly responsible for the observed decrease in the biosensor signal at some conditions (Fig. 4), it is more likely that steric stabilization plays an important role in the noted interference. Several other researchers have suggested that adsorption of NOM onto colloids (including *C. parvum* oocysts) may prevent colloid–surface interactions by a mechanism of steric stabilization (Franchi and O'Melia, 2003; Pelley and Tufenkji, 2008; Tufenkji et al., 2006). The organic acids may also interfere with *C. parvum* detection by masking antigen sites on the oocyst and/or binding sites on the immobilized layer of antibodies.

Latex microspheres are commonly used as model colloidal contaminants in studies related to water quality and treatment (Franchi and O'Melia, 2003; Li et al., 2004; Pelley and Tufenkji, 2008; Tufenkji et al., 2004). Suspensions of *C. parvum* (5×10^6 oocysts/mL) were mixed with latex colloids (1.5 μm; 5×10^6 particles/mL) and injected into the QCM-D flow chamber to evaluate the potential interference caused by the model colloidal contaminant. Values of f_{slope} and D_{slope} measured in the presence of the latex microspheres are presented in Fig. 6 along with the biosensor responses for *C. parvum* alone (10^7 oocysts/mL and 5×10^6 oocysts/mL). The latex colloids cause significantly more interference than the organic acids, resulting in decreases of 64% and 61% in f_{slope} and D_{slope}, respectively, when compared to the experiment with *C. parvum* alone.

3.3. *Cryptosporidium* detection in the presence of other biological agents

Water samples believed to be contaminated by an organism such as *C. parvum* may also contain a wide range of other organisms, including bacteria and viruses. Such organisms may cause interference during biosensing for the target

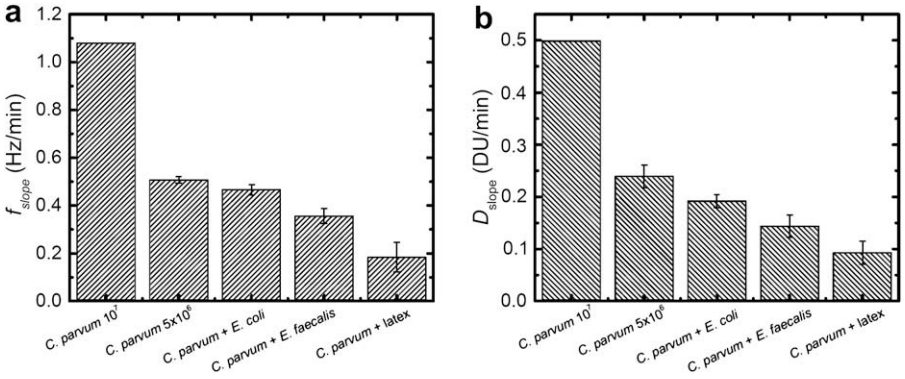

Fig. 6 – Average values of (a) f_{slope} and (b) D_{slope} measured during injection of: (i) 10^7 oocysts/mL in PBS alone, (ii) 5×10^6 oocysts/mL in PBS alone, (iii) 5×10^6 oocysts/mL in a mixture with *E. coli* O157:H7 (5×10^6 cells/mL), (iv) 5×10^6 oocysts/mL in a mixture with *E. faecalis* (5×10^6 cells/mL), and (v) 5×10^6 oocysts/mL in a mixture with 1.5 μm latex microspheres (5×10^6 particles/mL). Error bars correspond to 95% confidence intervals for at least 3 separate experiments.

parasite. The waterborne bacterial pathogens *E. coli* O157:H7 and *E. faecalis* were selected as representative Gram-negative and Gram-positive organisms, respectively, for evaluation of biosensor interference. When *E. coli* O157:H7 was injected alone onto the anti-*C. parvum* antibody functionalized biosensor surfaces, the measured f and D shifts were not distinguishable from the recognized instrument drift. It is also important to verify the biosensor response when *C. parvum* is mixed with bacteria. Values of f_{slope} and D_{slope} measured in the presence of either bacterium (5×10^6 cells/mL) are presented in Fig. 6. The data show that *E. coli* acts as a moderate interferent resulting in a decrease in the biosensor response; the value of f_{slope} decreased by 8% whereas D_{slope} decreased by 20% in the presence of *E. coli* O157:H7. The Gram-positive *E. faecalis* caused greater interference of the biosensor, resulting in a 30% decrease in f_{slope} and a 40% decrease in D_{slope} when compared to the experiment with *C. parvum* alone. The biosensor responses observed for the mixtures of bacteria and *C. parvum* suggest that the bacteria act as interferents even though they are not readily detected when injected alone into the biosensing flow modules. This result suggests that the bacteria may deposit onto the functionalized crystal surface, but not in large enough numbers to be detected. Although the deposited bacteria do not give rise to measurable changes in f or D when alone, they may affect detection of *C. parvum* by non-specifically binding to the crystal surface and thus effectively reducing (i.e., masking) the number of "free" antibody sites. This would explain the noted decrease in measured values of f_{slope} and D_{slope} in the presence of either bacterium (Fig. 6).

4. Conclusions

QCM-D was evaluated for detection of *C. parvum* via direct physisorption of antibodies onto gold-coated crystals. The initial f_{slope} and D_{slope} measured after injection of *C. parvum* yield similar linear working ranges (3×10^5–10^7 oocysts/mL) and rapid detection (~5 min) without sample preparation or concentration. When oocysts were injected in the presence of humic or fulvic acids, the biosensor response was sometimes negatively affected; likely as a result of steric stabilization or masking of antibodies and/or antigens. More significant interference was observed when *C. parvum* was mixed with colloids, either biological (*E. coli*, *E. faecalis*) or non-biological (latex microspheres). The model non-biological latex particles yielded the greatest extent of biosensor interference (64%) whereas the Gram-negative bacterium (*E. coli*) has a significantly lower effect (i.e., the biosensor response decreased by only 20%). The observed decrease in the biosensor response suggests that the mechanism of interference is one of non-specific colloid deposition onto the antibody covered crystal surface. The detection limit of the proposed QCM-D based biosensor is not as low as that reported by other researchers working with PEMC sensing devices. Moreover, the detection limit of this and most other sensors is significantly higher than typical environmental concentrations of *C. parvum* observed in surface waters (~1 oocyst/mL) (Ajeagah et al., 2007; Mons et al., 2009). Further studies are thus needed to significantly improve the biosensor response for parasite detection in complex water matrices containing lower oocyst numbers. Some techniques that may yield improved biosensor responses include (i) use of crystals with a higher fundamental resonance frequency, (ii) higher-density packing of the antibodies on the crystal surface and (iii) nanoparticle amplification. The results of this study underscore the importance of evaluating the potential interference of biosensors using both biological and non-biological agents.

Acknowledgements

This research was supported by NSERC (Discovery Grant and PGS awarded to C.P.), the Canada Research Chairs Program, the FQRNT Centre for Biorecognition and Biosensors (CBB), the Canadian Water Network (CWN), and the Canada Foundation for Innovation (CFI).

REFERENCES

Ajeagah, G., Njine, T., Foto, S., Bilong Bilong, C.F., Karanis, P., 2007. Enumeration of *Cryptosporidium* spp and *Giardia* spp (oo)cysts in a tropical eutrophic lake: the municipal lake of Yaounde. International Journal of Environmental Science and Technology 4 (2), 223–232.

Barbosa, J.M.M., Costa-de-Oliveira, S., Rodrigues, A.G., Hanscheid, T., Shapiro, H., Pina-Vaz, C., 2008. A flow cytometric protocol for detection of *Cryptosporidium* spp. Cytometry, Part A 73A (1), 44–47.

Campbell, G.A., Mutharasan, R., 2008. Near real-time detection of *Cryptosporidium parvum* oocyst by IgM-functionalized piezoelectric-excited millimeter-sized cantilever biosensor. Biosensors & Bioelectronics 23 (7), 1039–1045.

Campbell, G.A., Uknalis, J., Tu, S.I., Mutharasan, R., 2007. Detect of *Escherichia coli* O157:H7 in ground beef samples using piezoelectric excited millimeter-sized cantilever (PEMC) sensors. Biosensors & Bioelectronics 22 (7), 1296–1302.

Casemore, D.P., Wright, S.E., Coop, R.L., 1997. *Cryptosporidium* and Cryptosporidiosis. In: Fayer, R. (Ed.). CRC Press, Boca Raton, FL, pp. 65–92.

Dai, X., Hozalski, R.M., 2003. Evaluation of microspheres as surrogates for *Cryptosporidium parvum* oocysts in filtration experiments. Environmental Science & Technology 37 (5), 1037–1042.

Derjaguin, B.V., Landau, L.D., 1941. Theory of the stability of strongly charged lyophobic sols and of the adhesion of strongly charged particles in solutions of electrolytes. Acta Physicochimica URSS 14, 733–762.

Dolatshahi-Pirouz, A., Rechendorff, K., Hovgaard, M.B., Foss, M., Chevallier, J., Besenbacher, F., 2008. Bovine serum albumin adsorption on nano-rough platinum surfaces studied by QCM-D. Colloids and Surfaces B: Biointerfaces 66 (1), 53–59.

Edgar, R., McKinstry, M., Hwang, J., Oppenheim, A.B., Fekete, R.A., Giulian, G., Merril, C., Nagashima, K., Adhya, S., 2006. High-sensitivity bacterial detection using biotin-tagged phage and quantum-dot nanocomplexes. Proceedings of the National Academy of Sciences of the United States of America 103 (13), 4841–4845.

Fatisson, J., Domingos, R.F., Wilkinson, K.J., Tufenkji, N., 2009. Deposition kinetics of TiO_2 nanoparticles onto silica measured using QCM-D. Langmuir, in press.

Franchi, A., O'Melia, C.R., 2003. Effects of natural organic matter and solution chemistry on the deposition and reentrainment

of colloids in porous media. Environmental Science & Technology 37 (6), 1122–1129.
Green, R.J., Davies, J., Davies, M.C., Roberts, C.J., Tendler, S.J.B., 1997. Surface plasmon resonance for real time in situ analysis of protein adsorption to polymer surfaces. Biomaterials 18 (5), 405–413.
Hook, F., 1997. Development of a Novel QCM Technique for Protein Adsorption Studies. Department of Biochemistry and Biophysics and Department of Applied Physics, Chalmers University of Technology.
Hook, F., Kasemo, B., Nylander, T., Fant, C., Sott, K., Elwing, H., 2001. Variations in coupled water, viscoelastic properties, and film thickness of a Mefp-1 protein film during adsorption and cross-linking: a quartz crystal microbalance with dissipation monitoring, ellipsometry, and surface plasmon resonance study. Analytical Chemistry 73 (24), 5796–5804.
Hook, F., Rodahl, M., Brzezinski, P., Kasemo, B., 1998. Energy dissipation kinetics for protein and antibody–antigen adsorption under shear oscillation on a quartz crystal microbalance. Langmuir 14 (4), 729–734.
Hook, F., Voros, J., Rodahl, M., Kurrat, R., Boni, P., Ramsden, J.J., Textor, M., Spencer, N.D., Tengvall, P., Gold, J., Kasemo, B., 2002. A comparative study of protein adsorption on titanium oxide surfaces using in situ ellipsometry, optical waveguide lightmode spectroscopy, and quartz crystal microbalance/dissipation. Colloids and Surfaces B: Biointerfaces 24 (2), 155–170.
Jex, A.R., Smith, H.V., Monis, P.T., Campbell, B.E., Gasser, R.B., 2008. *Cryptosporidium* – biotechnological advances in the detection, diagnosis and analysis of genetic variation. Biotechnology Advances 26, 304–317.
Kang, C.D., Cao, C., Lee, J., Choi, I.S., Kim, B.W., Sim, S.J., 2008. Surface plasmon resonance-based inhibition assay for real-time detection of *Cryptosporidium parvum* oocyst. Water Research 42 (6–7), 1693–1699.
Kang, C.D., Lee, S.W., Park, T.H., Sim, S.J., 2006. Performance enhancement of real-time detection of protozoan parasite, *Cryptosporidium* oocyst by a modified surface plasmon resonance (SPR) biosensor. Enzyme and Microbial Technology 39 (3), 387–390.
Kim, J., Somorjai, G.A., 2003. Molecular packing of lysozyme, fibrinogen, and bovine serum albumin on hydrophilic and hydrophobic surfaces studied by infrared-visible sum frequency generation and fluorescence microscopy. Journal of the American Chemical Society 125 (10), 3150–3158.
Lee, S.H., Stubbd, D.D., Cairney, J., Hunt, W.D., 2005. Rapid detection of bacterial spores using a quartz crystal microbalance (QCM) immunoassay. IEEE Sensors Journal 5 (4), 737–743.
Li, X., Scheibe, T.D., Johnson, W.P., 2004. Apparent decreases in colloid deposition rate coefficients with distance of transport under unfavorable deposition conditions: a general phenomenon. Environmental Science & Technology 38, 5616–5625.
Lisle, J.T., Rose, J.B., 1995. *Cryptosporidium* contamination of water in the USA and UK – a minireview. Journal of Water Supply Research and Technology – Aqua 44 (3), 103–117.
Lubarsky, G.V., Davidson, M.R., Bradley, R.H., 2007. Hydration–dehydration of adsorbed protein films studied by AFM and QCM-D. Biosensors & Bioelectronics 22 (7), 1275–1281.
Mao, X., Yang, L., Su, X.L., Li, Y., 2006. A nanoparticle amplification based quartz crystal microbalance DNA sensor for detection of *Escherichia coli* O157:H7. Biosensors & Bioelectronics 21, 1178–1185.
Mons, C., Dumetre, A., Gosselin, S., Galliot, C., Moulin, L., 2009. Monitoring of *Cryptosporidium* and *Giardia* river contamination in Paris area. Water Research 43, 211–217.
Nimeri, G., Fredriksson, C., Elwing, H., Liu, L., Rodahl, M., Kasemo, B., 1998. Neutrophil interaction with protein-coated surfaces studied by an extended quartz crystal microbalance technique. Colloids and Surfaces B: Biointerfaces 11 (5), 255–264.
Pelley, A.J., Tufenkji, N., 2008. Effect of particle size and natural organic matter on the migration of nano- and microscale latex particles in saturated porous media. Journal of Colloid and Interface Science 321, 74–83.
Poitras, C., Tufenkji, N., 2009. A QCM-D based biosensor for *E. coli* O157:H7 highlighting the relevance of the dissipation slope as a transduction signal. Biosensors & Bioelectronics 24, 2137–2142.
Robinson, G., Watkins, J., Chalmers, R.M., 2008. Evaluation of a modified semi-automated immunomagnetic separation technique for the detection of *Cryptosporidium* oocysts in human faeces. Journal of Microbiological Methods 75 (1), 139–141.
Rose, J.B., 1997. Environmental ecology of *Cryptosporidium* and public health implications. Annual Review of Public Health 18, 135–161.
Sauerbrey, G.Z., 1959. The use of oscillators for weighing thin layers and for microweighing. Zeitschrift fur Physik 155, 2333–2336.
Shen, Z., Huang, M., Xiao, C., Zhang, Y., Zeng, X., Wang, P.G., 2007. Nonlabeled quartz crystal microbalance biosensor for bacterial detection using carbohydrate and lectin recognitions. Analytical Chemistry 79, 2312–2319.
Smith, H.V., 1992. *Cryptosporidium* and water – a review. Journal of the Institution of Water and Environmental Management 6 (4), 443–451.
Smith, J.E., Perdek, J.M., 2004. Assessment and management of watershed microbial contaminants. Critical Reviews in Environmental Science and Technology 34, 109–139.
Su, X.L., Li, Y., 2005. A QCM immunosensor for *Salmonella* detection with simultaneous measurements of resonant frequency and motional resistance. Biosensors & Bioelectronics 21 (6), 840–848.
Su, X.L., Li, Y., 2004. A self-assembled monolayer-based piezoelectric immunosensor for rapid detection of *Escherichia coli* O157:H7. Biosensors & Bioelectronics 19 (6), 563–574.
Subramanian, A., Irudayaraj, J., Ryan, T., 2006. A mixed self-assembled monolayer-based surface plasmon immunosensor for detection of *E. coli* O157:H7. Biosensors & Bioelectronics 21 (7), 998–1006.
Tencer, M., Charbonneau, R., Lahoud, N., Berini, P., 2007. AFM study of BSA adlayers on Au stripes. Applied Surface Science 253, 9209–9214.
Tufenkji, N., Dixon, D.R., Considine, R., Drummond, C.J., 2006. Multi-scale *Cryptosporidium*/sand interactions in water treatment. Water Research 40 (18), 3315–3331.
Tufenkji, N., Miller, G.F., Ryan, J.N., Harvey, R.W., Elimelech, M., 2004. Transport of *Cryptosporidium* oocysts in porous media: role of straining and physicochemical filtration. Environmental Science & Technology 38, 5932–5938.
Vaughan, R.D., O'Sullivan, C.K., Guilbault, G.G., 2001. Development of a quartz crystal microbalance (QCM) immunosensor for the detection of *Listeria monocytogenes*. Enzyme and Microbial Technology 29 (10), 635–638.
Verwey, E.J.W., Overbeek, J.T.G., 1948. Theory of the Stability of Lyophobic Colloids. Elsevier, Amsterdam.
Waswa, J., Irudayaraj, J., DebRoy, C., 2006. Direct detection of *E. coli* O157:H7 in selected food systems by a surface plasmon resonance biosensor. LWT – Food Science and Technology 40 (2), 187–192.
Wong, Y.Y., Ng, S.P., Ng, M.H., Si, S.H., Yao, S.Z., Fung, Y.S., 2002. Immunosensor for the differentiation and detection of *Salmonella* species based on a quartz crystal microbalance. Biosensors & Bioelectronics 17 (8), 676–684.